Radio Sky Mapping using System Temperatures of the EISCAT Svalbard Radar

L. Clausen

July 10, 2006

1 Introduction

It is a well known fact that the energy flux coming from the sky varies depending on the celestial pointing direction and the used frequency. In the plane of our galaxy the density of celestial objects is higher, thus the flux coming from this direction is higher than from the celestial poles. When scanning the sky at different frequencies, characteristic structures appear which allow assumptions about conditions at certain parts of our galaxy.

Incoherent scatter radars like the EISCAT Svalbard Radar (ESR) are in regular use to study phenomena occuring in the Earth's ionosphere, i.e. in altitudes between 100 and 1000km. As other radars the ESR logs its system temperature as an indicator for the system's health and thus the "goodness" of the recorded data. The system temperature is determined from the amplitude of noise inside the received signal. Since the two antennas of the ESR look essentially upwards into the sky, the system temperature is partly influenced by the sky's background radiation at the particular frequency used.

By studying the distribution of system temperatures in celestial coordinates of the ESR, a radar built for near-Earth observation can be turned into a radio telescope, measuring conditions lightyears away.

Using this technique, this study presents a map of the radio background radiation. Data covering 3 years of regular operations were used to generate the results presented here. The general characteristics of the radio background as determined by this approach are qualitatively compared with those derived from one special radio telescope study at a similar frequency.

Please note that results shown in this article are based on measurements of the systems temperature as an indicator for the goodness of data. The system temperature was not intended for the use of mapping the radio sky. However, the results show good accordance with one older study.

2 Calibration

Any signal is generally contaminated with noise. For convenience, when measuring electromagnetic radiation, the equivalent noise temperature corresponding to the power level at a certain frequency bandwidth is often considered. This temperature T equivalent to a noise power P_n is obtained by

$$P_n = k_B T \Delta\nu \tag{1}$$

where k_B is Boltzmann's konstant and $\Delta\nu$ is the frequency bandwidth. This, at an ohmic resistor translates to

$$V_n^2 = 4 k_B R T \Delta\nu \tag{2}$$

where V_n is the noise voltage and R is the resistance of the ohmic element.

System temperatures of antennas T_{sys} are measured by adding white noise of a well-known amplitude in pulses to the signal received. This is done before the raw signal undergoes any modification. From the difference between the signal amplitudes with and without artificially added noise and the knowledge of the zero line, the system temperature can be calculated.

Many factors influence the system temperature, therefore it can be looked at as a sum of contributions from different noise sources:

$$T_{sys} = T_{bg} + T_{sky} + T_{spill} + T_{loss} + T_{cal} + T_{rx} \tag{3}$$

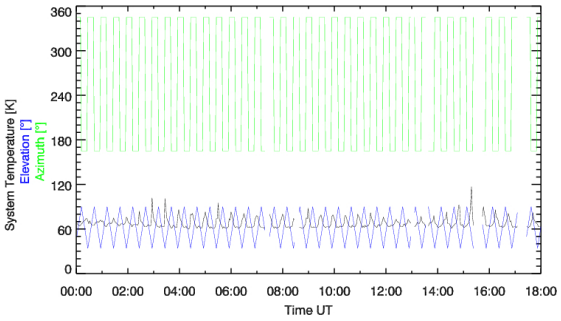

Figure 1: Typical measurement of the system temperature during the Common Program 3 on 9 Nov. 2005, along with the local pointing direction of the 32m antenna.

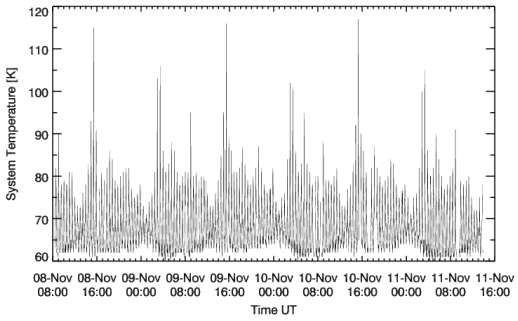

Figure 2: System temperature during a 3 1/2 day run of CP3 in November 2005.

where T_{bg} is the noise contribution from microwave and galactic backgrounds, T_{sky} is the noise contribution from atmospheric emission, T_{spill} is the noise contribution due to ground radiation (spillover and scattering), T_{loss} is the noise contribution due to losses in feed, T_{cal} is the noise contribution due to injected noise and T_{rx} is the receiver noise temperature.

In this study, the T_{bg} contribution to the total system temperature will be analysed in order to map the radio background radiation. To be able to relate changes in the system temperature to changes of T_{bg} in Equation (3) and thus changes in the background radiation, one must first make statements about the other contributions. In this study, they are, due to lack of precise knowledge, assumed to be constant at any pointing direction and at any time. This means that variations in the system temperature are assumed to only be caused by variations in the background radio flux. This seems a strong assumption but further investigation shows that the dominant part causing variations seems to be the sky.

Figure 1 shows an example for the typical system temperature during a Common Program 3 (CP3) measurement on 9 Nov. 2005. During this program the 32m antenna scans different elevations in a vertical plane - the sudden change in azimuth by 180° is caused by the antenna moving through the zenith position. After scanning 14 points along different elevations, the antenna is moved by 180° in azimuth to reach its original position. One sweep in completed in approximately 30 minutes. The dependence of the system temperature on the pointing direction of the 32m antenna is clearly observed.

If direct dependence of the noise level on local sources is assumed, the main part of the variations should be somehow connected to the variations of the (local) pointing position, i.e. the system temperature should oscillate with the same period as the local pointing direction. Clearly, the system temperature in Figure 1 shows this behaviour, however, when using different scaling and also include measurements from the entire 3 1/2 day run, an additional pattern emerges (see Figure 2)

It shows repeating features with larger periods which are unlikely to be caused by local sources. The system temperature peaks every day between 15:00 and 16:00 UT. A slighly less destinct maximum is reached every 24 hours between 03:00 nd 04:00 UT, i.e. 12 hours later than the maximum first mentioned. The variations in the noise level are minimal around 01:00 and 13:00 UT every day.

A frequency of $(12h)^{-1}$ indicates a dependence of the system temperature on the pointing direction relative to the Earth's rotational axis. In Figure 3 the pointing direction during this run is shown after transformation in celestial coordinates. Each measurement point is marked by a circle, changing colour from black over red to white, depending on the time of the measurement. The pointing directions at same elevations in the local coordinate system at different times are due to the rotation of the Earth around itself translated into a circular movement around the celestial pole. Thus, the pointing directions in celestial coordinates form a spiral which is skewed due to the non-parallelity of the Earth's rotation axis and the direction of the celestial poles.

Considering that radio sources are located at

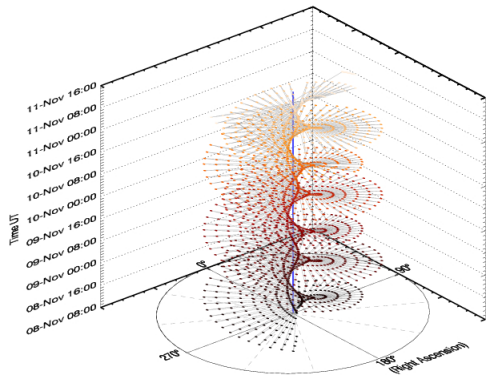

Figure 3: Pointing direction of the 32m antenna in celestial coordinates against time. Celestial elevation (Declination) in radial direction ranges from 90° to 0°, thus the black circle represents the celestial horizon. The position of the celestial North pole is marked with a blue line in polar coordinates.

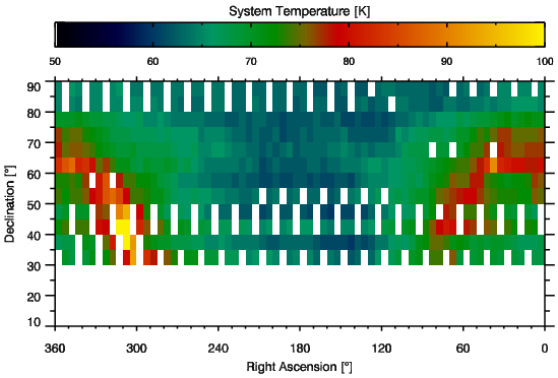

Figure 4: Same data as in Figure 2, pointing directions transformed into celestial coordinates and system temperatures averaged over 5° × 5° areas.

fixed celestial coordinates, the 24 hour rythm in detecting them due to higher background noise and thus higher system temperatures becomes apparent. Taking into account that our galaxy is a radio source forming a two-dimensional plane tilted against the rotational plane of the Earth around the Sun, the 12 hour rythm of elevated system temperature is obvious.

When transforming the pointing direction from local into celestial coordinates and coding the system temperature in colour, one obtains Figure 4. In Figure 4 the values have been averaged over an area of 5° × 5° which by no means reflects the antennas pointing accuracy or resolution. The sole reason was to enhance readability.

In the measurments the galactic plane shows up very nicely as part of a sinusodial signal. Even the fact that the energy flux is higher when looking at the galactic plane at around 300° Right Ascension (RA) then at 60° is detectable. This clearly indicates that the variations seen in Figure 1 are mainly due to the background radiation instead of local sources.

The statements made in this study are purely of qualitative nature. The offsets and their probable dependence on local pointing direction of the other contributions in Equation (3) are not known precicely enough to justify calculations of the actual energy flux.

3 Resolution

The ESR 32m antenna has a nominal pointing accurancy of less then 0.3°. However, when displaying data from this antenna, not the pointing accurancy but the resolution of the telescope is the limiting factor and determines an angular interval in which integration (averaging) of data is appropriate.

The resolution r, i.e. the minimal angular distance in radians of two still distinguishable objects, of any telescope is known from optics to be

$$r = 1.44\frac{\lambda}{D}. \tag{4}$$

In Equation (4) λ is the wavelength of the radiation and D denominates the diameter of the lense opening. D in case of the ESR is the diameter of the radar dish.

To get an upper limit for the resolution, the diameter was chosen to be that of the smaller antenna, i.e. 32m. Together with a wavelength of λ = 60cm at a frequency of 500MHz this yields

$$r = 1.31°. \tag{5}$$

Therefore the integration inteval was chosen to be 1.5° in both RA and declination (DEC).

4 Observations and Discussion

In Figure 5 the data availability in celestial coordinates is shown. The relatively few local Azimuth-Elevation directions covered by the

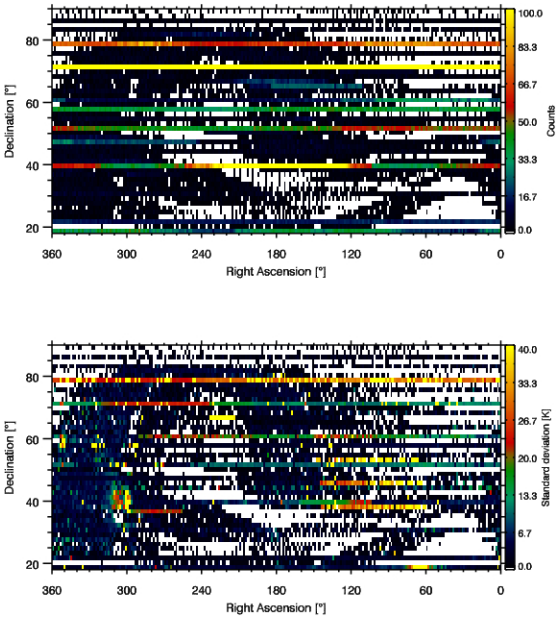

Figure 5: Data availability and stadard deviation for the ESR in celestial coordinates. White spaces indicate no data.

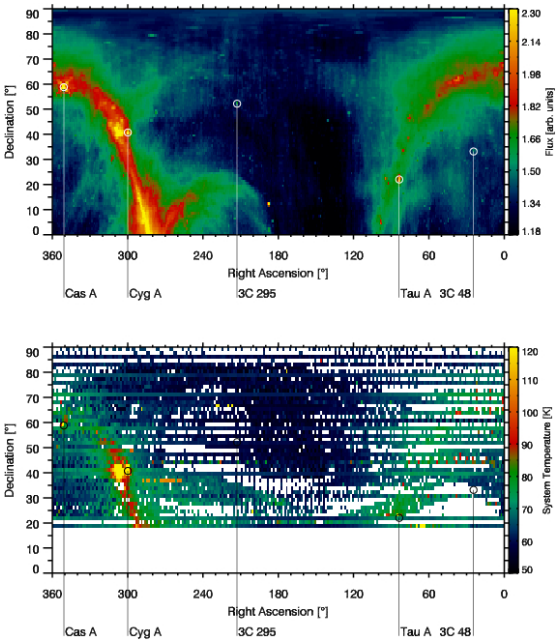

Figure 6: Comparisson between the data gathered by the 0408MHz survey (top panel) and the system temperature data from the ESR (bottom panel). White spaces indicate no data.

ESR are translated into a coverage of almost 50% of the sky in the interval RA $[0°, 360°]$ and DEC $[0°, 90°]$. A yellow line at all RA and just above 70° DEC is the result of the many times when measurements are made at a field aligned position, e.g. all measurments made with the 42m antenna. The different times of the year during which this happens are translated into all possible RA, however, the variation in DEC is very small ($\ll 1°$ at fixed pointing direction). Since the integration interval of this plot was 1.5°, these variations in DEC are eliminated. The same reasoning applies for the line around 40° DEC which originates from low elevation measurements.

Also shown in Figure 5 is the standard deviation of the system temperatures. If more than two measurements were found in an area of $1.5° \times 1.5°$, the standard deviation could be calculated.

The top panel of Figure 6 shows the radio background radiation as measured by the 0408Mhz survey from 1986 (see Haslam et al. 1982) in some arbitrary units with a logarithmic scale. The bottom panel shows the system temperatures linearly scaled and measured by the ESR radar at different celestial pointing directions. Also shown (in both panels) are the positions of 5 known significant radio sources and their names.

As discussed before the system temperature has been averaged over an area of $1.5° \times 1.5°$. If more than one measurement was found in an area, the median of those data has been plotted. This damps influence of very small and very big values and proved to produce more sensible results then the arithmetic average. The similarity between the two plots is good. The plane of the galaxy shows up nicely in the plot of the ESR data.

However, there is one intervalls in the data which shows unusual and significant high system temperatures: [36.5°, 38.0°] DEC and [255°, 290°] RA. The standard deviation in Figure 5 gives an explanation for the higher median in this intervall: because of a higher spread of relatively few (< 10) values in this intervall, the median is bigger than for comparable intervalls with lower standard deviation. This explains the reason for the relative high median value, however not the reason for the higher spread in the data. Also, the intervalls at RA [140°, 60°] and DEC [38.0°, 39.5°], [45.5°, 47.0°] and [53.0°, 54.5°] show even higher standard deviation with similarly low measurment numbers,

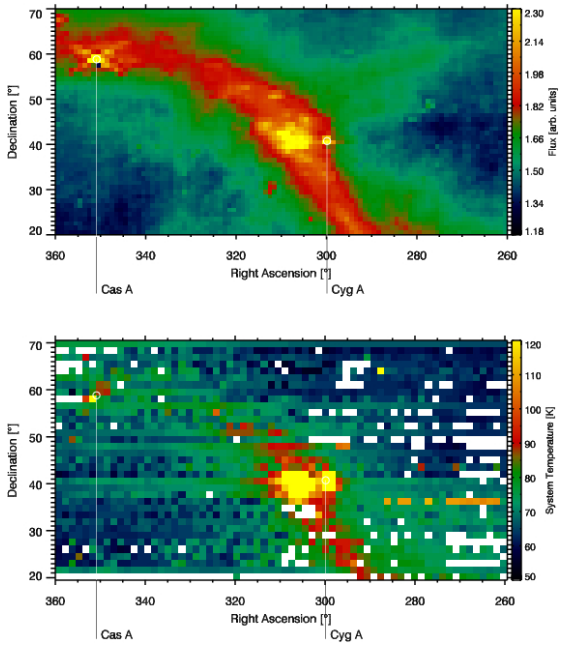

Figure 7: Zoom of Figure 6.

yet the median is of expected magnitude.

When looking at a zoom of the active region between [260°, 360°] RA and [20°, 70°] DEC (see Figure 7), one finds good qualitative accordance between the two surveys. The area around Cyg A in the ESR data is not as detailed as the 0408MHz data. Cas A is visible in the ESR data, yet not as significant.

5 Conclusion

This is a proof of concept, showing that it is possible to qualitatively map the radio background of the sky due to variations in the system temperature. Since the ESR was clearly not designed for this task, it has several drawbacks. It is difficult to make assumptions about the calibration of the data, i.e. which radio flux (in e.g. Jarns) corresponds to which system temperature. Also the resolution archieved with on 32m dish is limited. However, this study has shown that resonable results can be archieved.

References

C. G. T. Haslam, H. Stoffel, C. J. Salter, and W. E. Wilson. A 408 MHz all-sky continuum survey. II - The atlas of contour maps. *Astronomy and Astrophysics Supplement Series*, 47: 1–+, January 1982.